Impact of Fuselage Incidence on the Supersonic Aerodynamics of Two Fighter Configurations

Richard M. Wood* and David S. Miller*
NASA Langley Research Center, Hampton, Virginia

An experimental and theoretical investigation of fuselage-incidence effects on two fighter aircraft models, which differed in wing planform shape only, has been conducted in NASA Langley Research Center's Unitary Plan Wind Tunnel at Mach numbers 1.6, 1.8, and 2.0. Experimental and theoretical results were obtained on the two models with fuselage-incidence angles of 0, 2, and 5 deg. The fuselage geometry consisted of two side-mounted, flow-through, half-axisymmetric inlets and twin vertical tails. The two planforms tested were advanced cranked wings of 70/66 and 70/30 deg leading-edge sweep angles. The purpose of the study was to evaluate the effects of fuselage incidence on wing performance and to determine the ability of two linearized theory aerodynamic methods to predict these effects. Experimental data showed that fuselage incidence resulted in a positive increment in configuration lift and pitching moment; the majority of lift increment can be attributed to the fuselage-induced wing loading and the majority of the pitching moment increment to the fuselage loading. Theoretical analysis indicates that the PAN AIR and SDAS codes adequately predict the overall configuration forces and moments resulting from fuselage incidence, but the PAN AIR code predicted the distribution of forces and moments between the components more accurately.

Nomenclature

b	= wing span, in.
c	= wing chord, in.
$\bar{c}$	= wing mean aerodynamic chord, in.
C_D	= drag coefficient
$C_{D_{\min}}$	= minimum drag coefficient
ΔC_D	= change in drag coefficient, $(C_D - C_{D_{\min}})$
C_L	= lift coefficient
C_m	= pitching moment coefficient
$C_{m,0}$	= zero-lift pitching moment coefficient
c_r	= exposed root chord, in.
L/D	= lift-to-drag ratio
S	= wing reference area, in.^{2}
x	= longitudinal distance from model nose, in.
y	= spanwise distance from model centerline, in.
z	= vertical distance from wing mean chord plane, in.
α	= angle of attack, deg
δ	= fuselage-incidence angle, positive nose up, deg
ϵ	= wedge angle, deg

Subscripts

des	= design
fus	= fuselage
max	= maximum

Introduction

HISTORICALLY, fighter aircraft have been designed for efficient transonic cruise and maneuvering with little emphasis on sustained supersonic cruise capability. However, over the past several years, there has been considerable interest in a fighter aircraft that would have both supersonic cruise and maneuver capability. This type of aircraft would provide improved survivability in the increasingly hostile air combat environment of the future. As a result, military aircraft designers are placing more emphasis on sustained supersonic performance, while retaining superior cruise and maneuvering capability. The aerodynamic requirements within this expanded flight envelope are significant and the combination of these aerodynamic capabilities into an efficient airframe proves to be a challenging aerodynamic design problem.

Previous supersonic wing design studies[1,2] have proved satisfactory for wing-alone designs of supersonic transport-type configurations for which the interference effect of the other aircraft components forward of the wing are small and can be ignored. However, for fighter aircraft, the effect of the fuselage on the wing can be large and must be accounted for in the design of the wing camber. In an attempt to extend the wing-alone design approach to fighter aircraft, a fuselage camber requirement was defined that, when used, preserved the optimized wing-alone design characteristics.[3] Application of the wing-alone design approach, in conjunction with the fuselage camber requirement,[4,5] verified that efficient supersonic cruise performance levels could be obtained for fighter configurations; however, the resulting extreme fuselage camber was unrealistic for a multi-role fighter aircraft.

Since the wing-alone design studies, the wing design and optimization procedures[6] have been upgraded to include the effects of fuselage buoyancy and upwash.[7] Application of this new capability in the supersonic wing camber design method was performed in a more recent study[8] in which the wing design incorporated the fuselage buoyancy terms, but the wing and fuselage were orientated so that it was not necessary to include the effects of fuselage upwash.

The present experimental and theoretical investigation is an initial look at the effects of fuselage incidence (fuselage upwash) on wing and configuration performance. The supersonic wind tunnel model geometry consisted of a single fighter fuselage with two side-mounted flow-through inlets, twin vertical tails, and two interchangeable uncambered, cranked wings with 70/30 and 70/60 deg leading-edge sweep.

The purpose of the study was to evaluate the effect of fuselage upwash on wing performance and to evaluate the ability of two linear theory methods to predict those effects. The models were tested at Mach numbers 1.6, 1.8, and 2.0 in the NASA Langley Research Center's Unitary Plan Wind Tunnel. The paper reports the results of the experimental testing and theoretical analysis.

Received July 29, 1984; presented as Paper 84-2193 at the AIAA Applied Aerodynamics Conference, Seattle, Wash., Aug. 21-23, 1984; revision received Feb. 7, 1985. This paper is declared a work of the U.S. Government and therefore is in the public domain.

*Aero-Space Technologist, Fundamental Aerodynamics Branch, High-Speed Aerodynamics Division. Member AIAA.

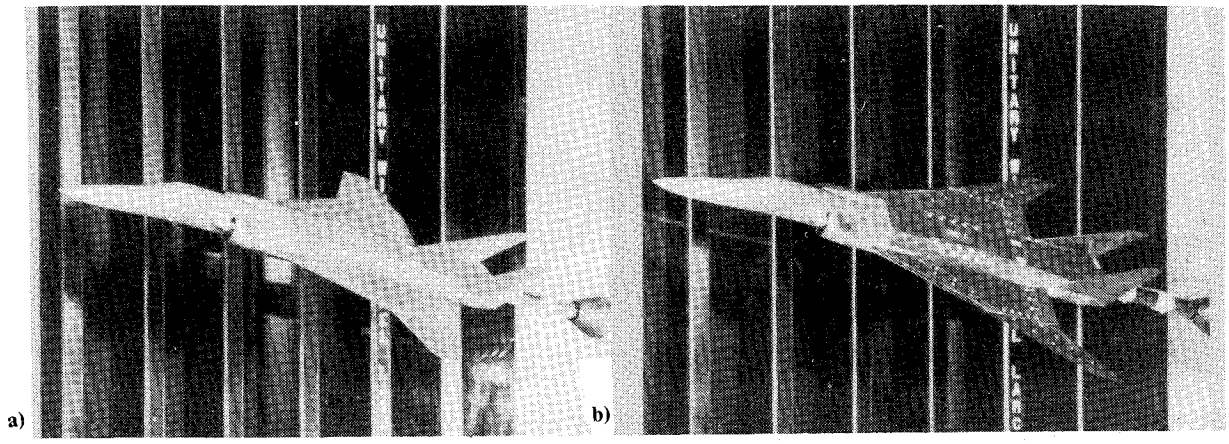

Fig. 1 Supersonic wind tunnel models: a) 70/30 deg crank wing; b) 70/66 deg crank wing.

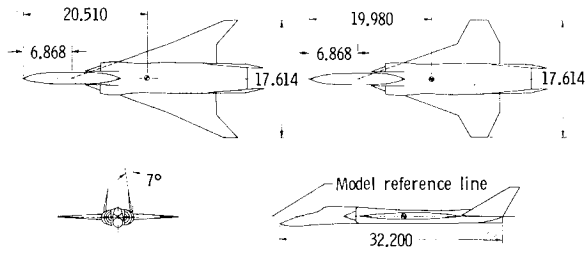

Fig. 2 Three-view sketch of supersonic wind tunnel models.

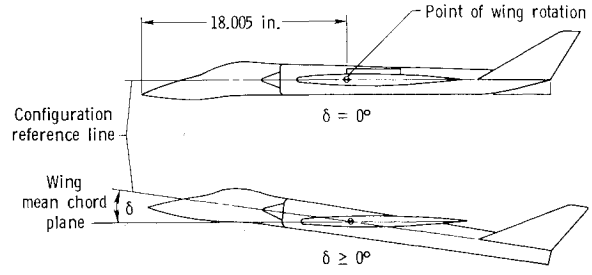

Fig. 3 Details of fuselage incidence.

Model Description

The two wind tunnel models tested were 4% scale representations of an advanced fighter aircraft concept. The models consisted of a single fighter fuselage with side-mounted, flow-through, half-axisymmetric inlets, twin vertical tails, and two uncambered wings that varied in planform shape only. The two planforms tested were a 70/30 deg crank wing and a 70/66 deg crank wing. The two planforms were selected in an aircraft sizing study discussed in Ref. 9; the initial supersonic testing of these models was reported in Ref. 10.

Figure 1 shows the two advanced-fighter configuration models installed in test section 1 of the Langley Unitary Wind Tunnel. Three-view sketches of the two models are shown in Fig. 2.

The relative incidence between the fuselage and wing for experimental testing was created by inserting a wedge between the fuselage wing-attachment pad and wing-attachment tab. The point of wing rotation and the definition of the fuselage-incidence angle δ are shown in Fig. 3. The approach used to produce fuselage incidence resulted in a significant amount of fuselage uppersurface distortion, which did significantly impact the experimentally measured minimum drag values for each configuration. However, these body distortions should have a negligible effect on the drag-due-to-lift values measured experimentally.

Discussion

An experimental and theoretical investigation of the near-field interference effects induced by rotating the fuselage to a positive incidence relative to the wing mean chord plane has been conducted. Experimental testing was performed on two advanced-fighter configurations, which differed in wing planform only, at fuselage-incidence angles of 0, 2, and 5 deg. Theoretical analysis was directed at determining the capability of two linearized theory methods to predict the experimentally measured effects. In addition to the discussion of the experimental results and theoretical analysis, a discussion on the impact of fuselage upwash on supersonic wing camber design for fighter aircraft is also presented.

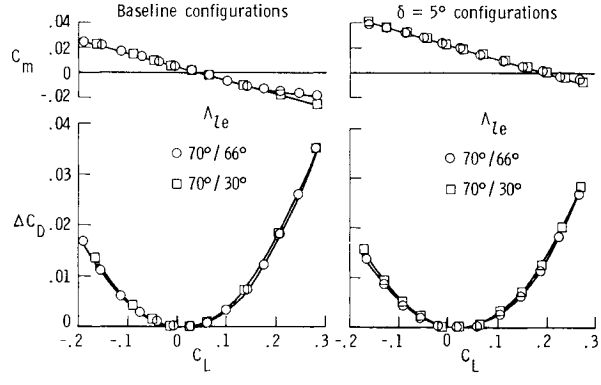

Fig. 4 Effect of planform on the experimentally measured drag due to lift and pitching moment at $M = 1.80$.

Experimental Results

High-speed wind tunnel tests were performed over a Mach number range of 1.6-2.0, at a Reynolds number of 2×10^6/ft, and at angles of attack from -4 to 20 deg. Test results for the two configurations are presented at a Mach number of 1.80 for fuselage-incidence angles of 0, 2, and 5 deg, with a special emphasis on the 70/66 deg crank-wing configuration. Drag data are presented as an incremental change from the minimum drag value of each configuration. All data have been reduced with respect to the wing reference plane.

From the data presented in Fig. 4, a comparison of the drag and pitching moment characteristics can be made for the two configurations at fuselage-incidence angles of 0 and 5 deg. Comparing the pitching moment characteristics of the two configurations with a fuselage incidence of 0 deg reveals that the 70/30 deg crank-wing geometry remains linear out to a 0.3

lift coefficient, but the 70/66 deg crank-wing geometry has an unstable break at 0.15 lift coefficient. As previously discussed in Ref. 10, this break in pitching moment for the 70/66 deg crank wing is a result of extensive upper-surface flow separation occurring on the outboard wing panel at 4 deg angle of attack. A comparison of the drag characteristics for the two configurations at 5 deg fuselage incidence angle shows that the 70/66 deg crank-wing configuration is still outperforming the 70/30 deg crank-wing configuration at the low-to-moderate lift conditions.

Presented in Fig. 5 are the effects of fuselage incidence on the drag and pitching moment characteristics of the 70/30 and 70/66 deg crank-wing configurations. The pitching moment data for the 70/30 deg configuration indicate that a change in fuselage incidence from 0 to 5 deg produced an 0.016 increment in $C_{m,0}$; however, neither the stability level nor the linearity of the $C_m - C_L$ curves were affected. The drag characteristics of the 70/30 deg crank-wing configuration show that an increase in fuselage incidence from 0 to 5 deg results in a 15% reduction in the cruise ($C_L = 0.1$) drag due to lift and a 5 – 10% reduction in drag due to lift at moderate lift coefficients ($C_L = 0.2 - 0.3$). In addition to the 0 and 5 deg fuselage-incidence angles, the 70/66 deg crank wing was also tested with 2 deg of fuselage incidence. In Fig. 5, the pitching moment data show that 2 deg of fuselage incidence produced a 0.007 increment in $C_{m,0}$ and 5 deg of fuselage incidence produced a 0.018 increment in $C_{m,0}$, which is comparable to that seen for the 70/30 deg crank-wing configuration. However, unlike the 70/30 deg crank-wing data, changing the fuselage incidence for the 70/66 deg crank wing did alter the linearity of the $C_m - C_L$ curve. The data show that changing from 0 to 5 deg of fuselage incidence extended the linear range of the pitching moment an additional 0.075 in lift coefficient. These data suggest that fuselage incidence can be used to delay wing upper-surface flow separation. The drag characteristics for the 70/66 deg crank wing with 0, 2, and 5 deg of fuselage incidence show results similar to those observed for the 70/30 deg crank wing. At the cruise lift condition ($C_L = 0.1$), a 25% improvement in induced drag is seen and a moderate lift coefficients ($C_L = 0.2 - 0.3$), 5 – 10% improvement is realized for 5 deg of fuselage incidence. The data for 2 deg of fuselage incidence also show reductions in drag due to lift out to $C_L = 0.30$; however, the magnitudes are approximately half those obtained for the 5 deg fuselage-incidence case.

For the 70/66 deg wing configuration, the effects of fuselage incidence on the lifting and pitching moment characteristics are given in Fig. 6 and the corresponding upper-surface flow quality is examined using the oil flow photographs presented in Fig. 7. The lift data show that 5 deg of fuselage incidence results in approximately a 0.075 increase in lift coefficient for any given wing angle of attack. However, the data also show that for both 0 and 5 deg fuselage incidence, flow separation is occurring at approximately 4 deg angle of attack; this corresponds to lift coefficients of 0.15 for 0 deg of fuselage incidence and 0.23 for 5 deg of fuselage incidence. The onset of flow separation occurring at 4 deg angle of attack, regardless of fuselage-incidence angle, can also be seen in the pitching moment data of Fig. 6. These effects can be further substantiated by investigating the quality of the flow on the wing upper surface. Presented in Fig. 7 are oil flow photographs of the 70/66 deg crank wing with 0 and 5 deg of fuselage incidence. Comparing the photographs for 0 deg of fuselage incidence (top row) to those for 5 deg of fuselage incidence (bottom row) reveals that the configuration with 5 deg of fuselage incidence requires approximately 2 deg less angle of attack in order to obtain the same wing upper-surface flow characteristics and lift coefficient. This indicates that the fuselage at 5 deg of incidence is inducing a spanwise upwash distribution comparable to an upwash field of a 2 deg angle of attack. The photographs show that for 0 deg of fuselage incidence the flow has begun to separate at a $C_L = 0.15$ ($\alpha = 4$ deg); however, for 5 deg of fuselage incidence, the flow is still attached at $C_L = 0.161$ ($\alpha = 2$ deg). The photographs also show that at 6 deg angle of attack for

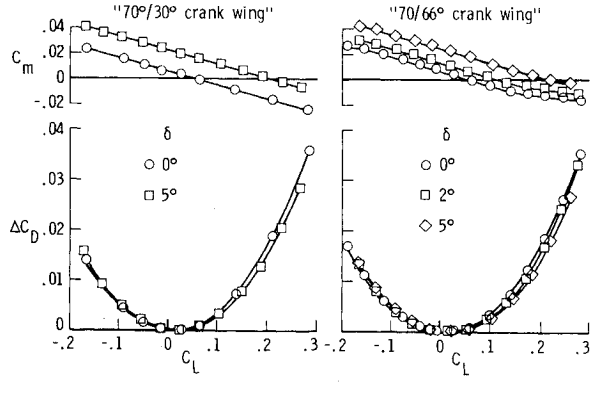

Fig. 5 Effect of fuselage incidence on the experimentally measured drag due to lift and pitching at $M = 1.80$.

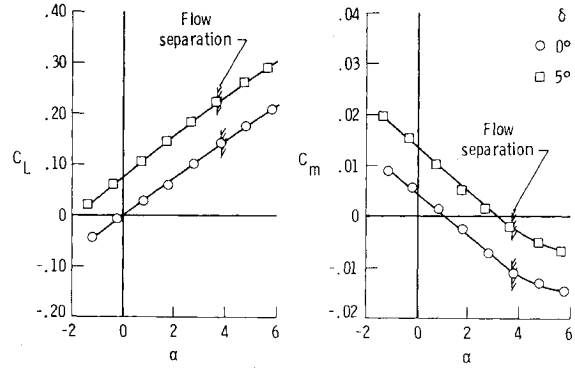

Fig. 6 Effect of fuselage incidence for the 70/66 deg crank-wing configuration on the experimentally measured lift and pitching moment at $M = 1.80$.

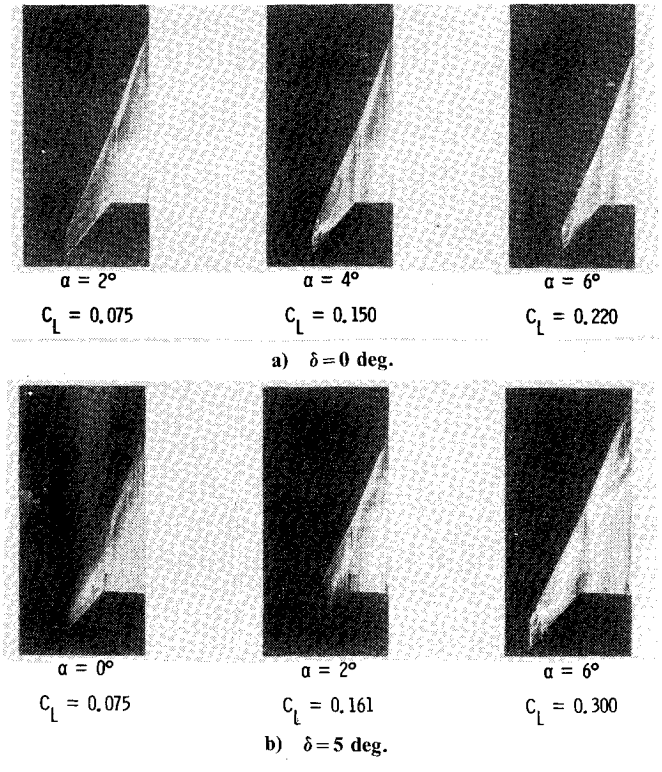

Fig. 7 Oil flow photographs for the 70/66 deg crank-wing configuration at $M = 1.80$.

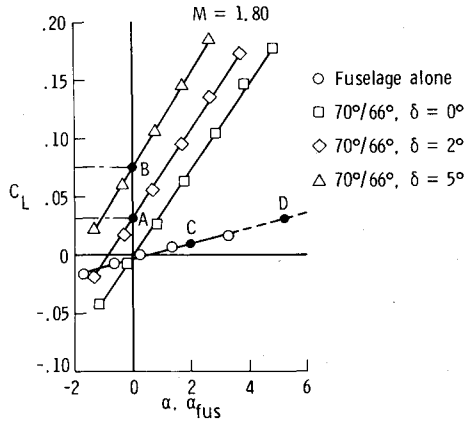

Fig. 8 Evaluation of the lifting characteristics for the 70/66 deg crank-wing configuration at $M = 1.80$.

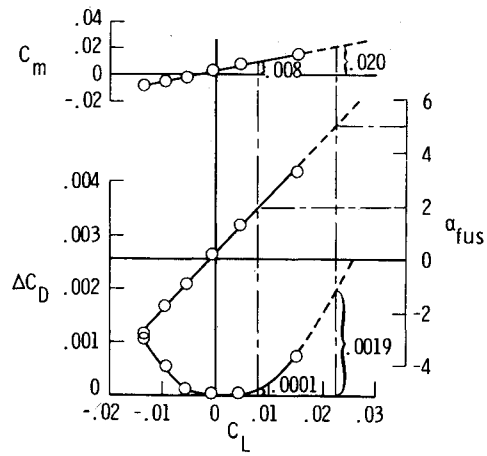

Fig. 9 Longitudinal aerodynamics of the fuselage at $M = 1.80$.

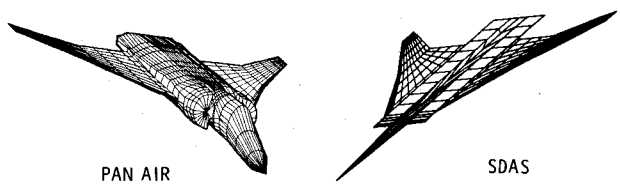

Fig. 10 Computer graphics of theoretical models.

both 0 and 5 deg of fuselage incidence, similar flow separation conditions have occurred. The correlation between the force and moment data of Fig. 6 and the oil flow photographs of Fig. 7 is consistent and indicates that both the wing lifting efficiency and flow quality are improved by inclining the fuselage at a positive incidence relative to the wing. In addition to providing a positive induced-lift increment, positive fuselage incidence also provided a positive increment in zero-lift pitching moment.

The distribution of lift between the wing and fuselage can be determined by comparing the lift at points A and B (70/66 deg crank-wing configuration) to the lift at points C and D (fuselage alone), respectively. See Fig. 8. Concentrating on the 70/66 deg crank-wing data at an angle of attack of 0 deg, it can be seen that 2 deg of fuselage incidence produced an increment in lift coefficient of approximately 0.03 (point A) and 5 deg of fuselage incidence produced an increment in lift coefficient of approximately 0.075 (point B). The fuselage along data show that at an angle of attack of 2 deg the fuselage has a lift coefficient of 0.008 (point C) and at 5 deg it has a lift coefficient of 0.022 (point D). By comparing the lift data for the total configuration and for the fuselage alone, where the fuselage is at 2 deg (points A and C) and at 5 deg (points B and D), it can be concluded that the fuselage is carrying only

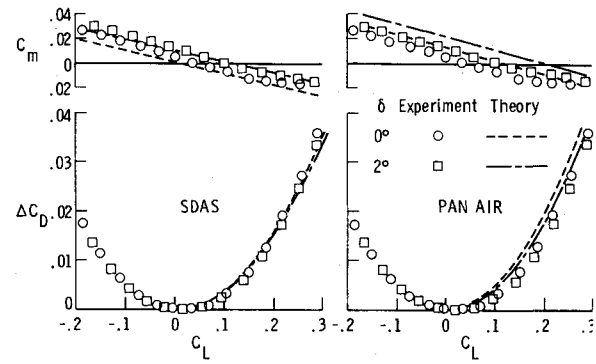

Fig. 11 Comparison between measured and predicted drag due to lift and pitching moment characteristics of the 70/66 deg crank-wing configuration at $M = 1.80$.

28% of the total configuration lift. The remaining 72% is wing lift induced by the fuselage upwash. On the basis of the lift data of Fig. 8, the flow visualization data of Fig. 7, and the previously discussed drag-due-to-lift data, we conclude that fuselage incidence does improve the lifting efficiency of a highly swept wing.

Presented in Fig. 9 are the fuselage-alone longitudinal characteristics. As previously shown in Fig. 5 for the 70/66 deg crank-wing configuration, a 2 deg fuselage incidence produced a 0.008 increment in $C_{m,0}$ and a 5 deg fuselage incidence produced an 0.020 increment in $C_{m,0}$. The fuselage-alone pitching moment data closely match these levels of pitching moment at both 2 and 5 deg angles of attack. The drag characteristics for the fuselage alone reveal that varying fuselage angle of attack between -1 and $+2$ deg results in essentially no change (ΔC_D less than 0.0001) in the minimum drag level. However, at an angle of attack of 5 deg, the isolated fuselage would be expected to produce an increase in minimum drag coefficient of at least 0.0019, which could neutralize any improvements in wing performance. Analysis of the fuselage-alone data has shown that the total $C_{m,0}$ increment and 28% of the lift increment can be attributed to the fuselage. In addition, the data show that no significant minimum drag penalties result with small amount of fuselage incidence, i.e., $\alpha_{fus} \leq 2$ deg.

Theoretical Analysis

Two linearized theory supersonic aerodynamic prediction techniques were selected for performing the theoretical analysis. The methods chosen were the PAN AIR code[11] and the lift analysis method of Ref. 6 as implemented in the supersonic design and analysis system (SDAS).[7]

The PAN AIR code is an advanced panel method that employs surface distributions of quadratically varying doublet and linearly varying source distributions for computing the surface flow properties and resultant forces and moments. This code has the capability to analyze completely arbitrary configurations; however, considerable attention must be paid to the details of the intersection of component boundaries, which results in a complicated geometric modeling process. The theoretical model defined for all PAN AIR analysis is shown in the left portion of Fig. 10 and consists of an exact representation of the fuselage geometry and a zero-thick wing.

The wing analysis method of Ref. 6 has been coupled with several fuselage definition options that may be used in performing the lift analysis with the SDAS code. A sensitivity study was conducted to determine the best option to use for representing the fuselage geometry and a mean chord plane representation of both the fuselage and wing planform was selected for the SDAS analysis. Shown in the right portion of Fig. 10 is the theoretical model used for all SDAS analysis.

A review of the previously presented experimental force and moment data showed that positive increments in lift and pitching moment can be obtained with little or no drag penalty for fuselage angles of attack less than 2 deg and that, at these low fuselage angles of attack, the linear theory assumption of the two analysis methods should not be violated. For these reasons, the following theoretical analysis will be restricted to the 2 deg fuselage-incidence condition.

Presented in Fig. 11 are typical theoretical and experimental force and moment results for the 70/66 deg configuration with 0 and 2 deg of fuselage incidence. The SDAS lift analysis results shown in Fig. 11 are in good agreement with the experimentally measured drag and pitching moment characteristics, but incorrectly predict the stability level and drag increment due to fuselage incidence. The PAN AIR results presented in Fig. 11 correctly predict the experimentally measured increments in drag and pitching due to fuselage incidence, but incorrectly predict the absolute levels of both.

Presented in Fig. 12 is a comparison of predicted lifting characteristics of the two methods for the 70/66 deg crank-wing configuration with 2 deg fuselage incidence. The lift curve data show that both methods accurately predict the lift of the complete configuration, but only PAN AIR accurately predicts the fuselage-alone lift characteristics. A breakdown of the total configuration lift forces predicted by each theoretical method into fuselage and wing lift is shown on the bar graph at the right of Fig. 12. The breakdown of theoretical lift at $\alpha = 0$ deg has been extracted from the computational results using the spanwise lift distributions of the wing and fuselage. The underprediction of the fuselage-alone lift by the SDAS code is not observed in the bar graph. The bar graph data show that the SDAS code predicts an even distribution of the lift force between the wing and the fuselage; however, the PAN AIR code predicts the same distribution of lift between the fuselage and wing as was experimentally measured. The experimental precent of wing lift was determined by taking the difference between the fuselage-alone data and the data for the complete configuration.

The theoretical results indicate that both methods are adequate for aerodynamic analysis purposes, but that the PAN AIR code is much better at predicting the individual fuselage and fuselage-induced effects associated with fuselage incidence.

Design Application

Existing supersonic wing camber design procedures have been proved adequate for wing-alone and supersonic transport-type configurations[1] in which the near-field interference effects of the various components can be neglected when compared to the wing aerodynamics. In contrast, a fighter-type fuselage can have a significant impact on wing aerodynamics and the application of wing-alone methods to fighter aircraft can result in an extensive modification to the fuselage geometry.[4] Because of the limited scope of previous methods and the increased attention to the supersonic efficiency of fighter aircraft, the wing-alone camber design methodology of Ref. 6 was modified to include configuration-related loadings and surface-ordinate constraints.[7] The configuration-related loadings account for fuselage upwash, fuselage buoyancy, and nacelle pressure fields. However, attempts to employ the existing design methods for the application of fuselage-incidence effects have been unsuccessful. The failure of the design method can be attributed to the inability of the lift analysis method of Ref. 7 to predict accurately the fuselage-alone aerodynamics and fuselage-induced flowfield.

Depicted in Fig. 13 are the two basic components of a new wing-camber design approach, PAN AIR, and the SDAS wing camber design methodology of Ref. 7. This new approach, initially alluded to in Ref. 9, employs the PAN AIR code for computing the fuselage aerodynamic characteristics and the

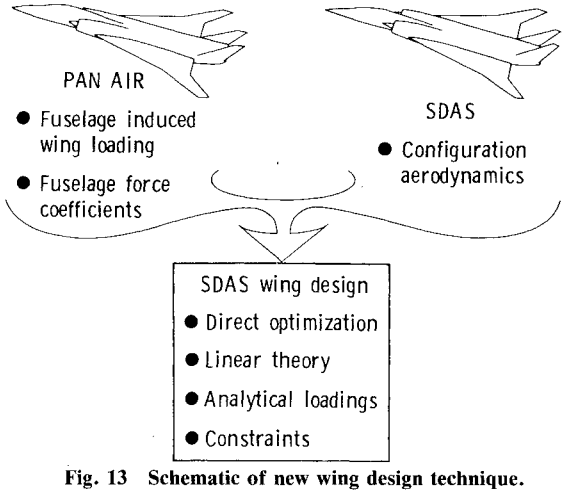

Fig. 13 Schematic of new wing design technique.

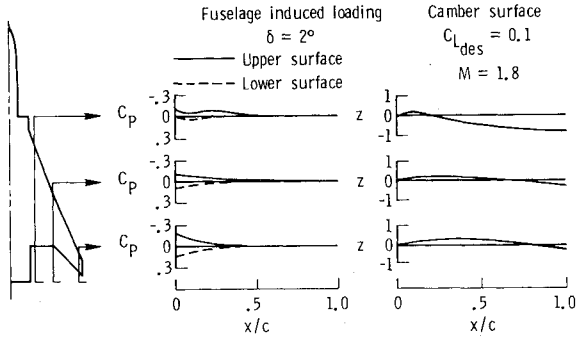

Fig. 14 Results of new wing design technique.

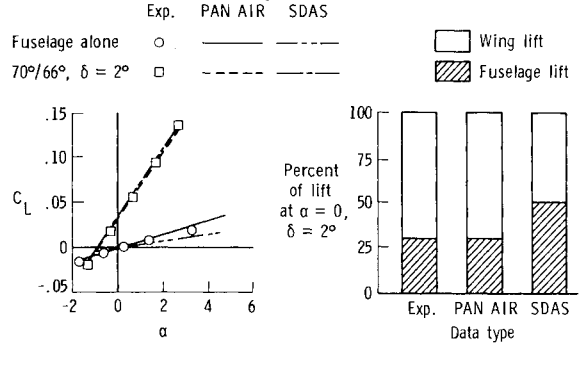

Fig. 12 Breakdown of the measured and predicted lift of the 70/66 deg crank/wing configuration at $M = 1.80$.

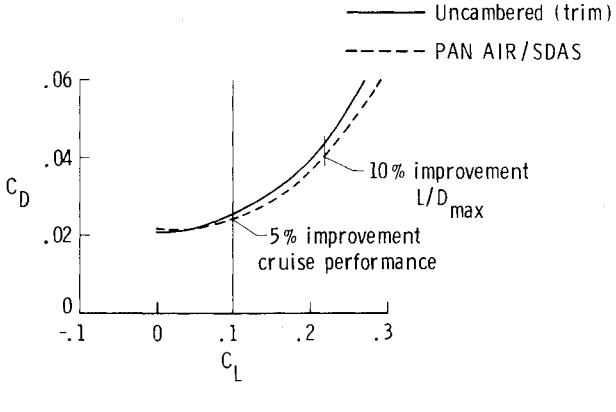

Fig. 15 Evaluation of new wing design technique.

fuselage-induced interference effects on the wing. These PAN AIR-predicted effects, shown in Fig. 14, are incorporated into the SDAS wing-optimization procedures as an aerodynamic wing loading. Initial application of this new wing design approach will be for the 70/66 deg crank-wing configuration with 2 deg of fuselage incidence. A representative camber surface from the new combined approach is shown on the right of Fig. 14. In this design case, appropriate design constraints were employed for trimmed flight at $M=1.80$. Figure 15 shows the theoretical drag predictions of the new camber design and the uncambered 70/66 deg crank-wing trimmed drag polar. The combined approach provides improved performance at $C_L=0.10$ of 5% and at $(L/D)_{max}$ of 10%.

Conclusions

An experimental and theoretical investigation of the effects of fuselage incidence has been conducted in the NASA Langley Research Center's Unitary Plan Wind Tunnel at Mach numbers 1.6, 1.8, and 2.0. The supersonic data were obtained for fuselage incidence angles of 0, 2, and 5 deg. Experimental results showed that fuselage incidence provided a positive increment in both lift and pitching moment, with the majority of the lift increment being attributed to the fuselage-induced upwash acting on the wing and the majority of the pitching moment increment attributed to the fuselage effects. In addition, an analysis of the data indicated that these positive lift and pitching moments effects can be achieved with no significant minimum drag penalty. Evaluation of the theoretical prediction capability revealed that both SDAS and PAN AIR accurately predicted the overall lift and moment increments due to fuselage incidence; however, the PAN AIR code better predicted the aerodynamics of the fuselage and the fuselage-induced effects. These effects can have a large impact on the design of a supersonic wing camber surface. To address the importance of fuselage incidence on wing camber design, a theoretical study was conducted in which the fuselage-induced aerodynamics predicted by the PAN AIR code were combined with the wing camber design capability of the SDAS code. This study showed that a much more realistic camber surface would result.

References

[1]*Proceedings from Conference on Technology for Supersonic Cruise Military Aircraft,* U.S. Air Force Wright Aeronautical Laboratories, Wright-Patterson AFB, Ohio, 1976.

[2]*Proceedings from Conference on Operational Utility of Supersonic Cruise,* U.S. Air Force Wright Aeronautical Laboratories, Wright-Patterson AFB, Ohio, 1977.

[3]Dollyhigh, S. M., Morris, O. A., and Adams, M. S., "Experimental Effect of Fuselage Camber on Longitudinal Aerodynamic Characteristics of a Series of Wing-Fuselage Configurations at a Mach Number of 1.41," NASA TM X-3559, 1977.

[4]Shrout, B. L., "Aerodynamic Characteristics at Mach Numbers from 0.6 to 2.16 of a Supersonic Cruise Fighter Configuration with a Design Mach Number of 1.8," NASA TM X-3559, 1977.

[5]Morris, O. A., "Subsonic and Supersonic Aerodynamic Characteristics of a Supersonic Cruise Fighter Model with a Twisted and Cambered Wing with 74° Sweep," NASA TM X-3530, 1977.

[6]Carlson, H. W., and Miller, D. S., "Numerical Methods for the Design and Analysis of Wings at Supersonic Speeds," NASA TN D-7713, Dec. 1974.

[7]Middleton, W. D., Lundry, J. L., and Coleman, R. G., "A System for Aerodynamic Design and Analysis of Supersonic Aircraft, Pt. 2: User's Manual," NASA CR-3352, 1980.

[8]Miller, D. S. and Schemensky, R. T., "Design Study Results of a Supersonic Cruise Fighter Wing," AIAA Paper 79-0062, Jan. 1979.

[9]Wood, R. M., Miller, D. S., Hahne, D. E., Niedling, L., and Klein, J., "Status Review of a Supersonically Biased Fighter Wing-Design Study," AIAA Paper 83-1857, July 1983.

[10]Wood, R. M. and Miller, D. S., "Investigation of Wing Planform Effects at Supersonic Speeds for an Advanced-Fighter Configuration," NASA TP-2269, 1984.

[11]Moran, J., Tinoco, E. N., and Forrester, T. J., "User's Manual, Subsonic/Supersonic Advanced Panel Pilot Code," NASA CR-152047, 1978.